Version of January 15, 2021

Structure-preserving Gauss methods for the nonlinear Schrödinger equation

Georgios Akrivis · **Dongfang Li**

Received: June 17, 2020 / Accepted: March 2, 2021

Abstract We use the scalar auxiliary variable (SAV) reformulation of the nonlinear Schrödinger (NLS) equation to construct structure-preserving SAV–Gauss methods for the NLS equation, namely L^2-conservative methods satisfying a discrete analogue of the energy (the Hamiltonian) conservation of the equation. This is in contrast to Gauss methods for the standard form of the NLS equation that are L^2-conservative but not energy-conservative. We also discuss efficient linearizations of the new methods and their conservation properties.

Keywords Nonlinear Schrödinger equation · Gauss methods · scalar auxiliary variable approach · structure-preserving methods · L^2-conservative methods · energy-conservative methods · linearly implicit schemes · continuous Galerkin method

Mathematics Subject Classification (2000) 65M12 · 65M60 · 35Q41

1 Introduction

Let $\Omega \subset \mathbb{R}^d$ be a bounded domain with smooth boundary $\partial\Omega$, and consider the following initial and boundary value problem for the nonlinear Schrödinger (NLS) equation with power nonlinearity: seek a complex-valued function $u : \bar{\Omega} \times [0,T] \to \mathbb{C}, u = u(x,t)$, satisfy-

The work of Dongfang Li was partially supported by NSFC (No. 11771162).

Georgios Akrivis
Department of Computer Science and Engineering, University of Ioannina, 451 10 Ioannina, Greece, and Institute of Applied and Computational Mathematics, FORTH, 700 13 Heraklion, Crete, Greece
Tel.: +30-26510-08800
E-mail: akrivis@cse.uoi.gr

Dongfang Li
School of Mathematics and Statistics, Huazhong University of Science and Technology, Wuhan 430074, China, and Hubei Key Laboratory of Engineering Modeling and Scientific Computing, Huazhong University of Science and Technology, Wuhan 430074, China
E-mail: dfli@mail.hust.edu.cn

ing

$$\begin{cases} u_t = \mathrm{i}\Delta u + \mathrm{i}\lambda |u|^{p-1}u & \text{in } \Omega \times [0,T], \\ u = 0 & \text{on } \partial\Omega \times [0,T], \\ u(\cdot,0) = u^0 & \text{in } \bar{\Omega}, \end{cases} \tag{1.1}$$

where λ is a nonzero real number, u^0 is a given complex-valued function, and $p > 1$.

Two fundamental invariance properties of the NLS equation are the conservations of the L^2-norm, i.e., of the charge, density or mass, depending on the application, and of the energy (Hamiltonian) $E(u(\cdot,t))$, here multiplied by 2 for convenience,

$$\begin{cases} I(u(\cdot,t)) := \|u(\cdot,t)\|^2 = \|u^0\|^2, \\ E(u(\cdot,t)) := \|\nabla u(\cdot,t)\|^2 - \dfrac{2\lambda}{p+1}\|u(\cdot,t)\|_{L^{p+1}}^{p+1} = E(u^0), \end{cases} \qquad 0 \leqslant t \leqslant T, \tag{1.2}$$

with $\|\cdot\|$ and $\|\cdot\|_{L^{p+1}}$ the $L^2(\Omega)$- and $L^{p+1}(\Omega)$-norms.

It is well known that the Gauss methods for the standard form (1.1) of the NLS equation are L^2-conservative, [2,23], but are *not* energy-conservative. In this article, we use the scalar auxiliary variable (SAV) reformulation of the NLS equation to construct classical, L^2-conservative SAV–Gauss methods satisfying a discrete analogue of the energy conservation property. To emphasize the basic construction technique and to keep the article at a reasonable length, we do not study convergence properties of the SAV–Gauss methods. We note that the analysis proceeds along the lines of [23], [3] or [4], depending on the variant of the method; cf. Remark 4.1.

The NLS equation is one of the most important equations in mathematical physics; it is used in nonlinear optics [38, Chapter 1], in fiber optics communications [1], in plasma physics [30], in geophysics [29], and in mathematical biology [27]. See also the survey [31]. We refer to [38] and [35,36] for various properties of the NLS equation and for further references. For the *cubic* NLS and $\Omega \subset \mathbb{R}^2$ with smooth boundary $\partial\Omega$, it is proved in [9] that the initial and boundary value problem (1.1) possesses a unique global solution in $H^2(\Omega)$, provided $u^0 \in H^2(\Omega) \cap H_0^1(\Omega)$ and either $\lambda < 0$ or $\lambda > 0$ and $c_0\lambda\|u^0\|^2 < 2$, with c_0 a positive constant occurring in the Gagliardo–Nirenberg inequality,

$$\forall v \in H_0^1(\Omega) \quad \|v\|_{L^4(\Omega)}^4 \leqslant c_0\|v\|^2\,\|\nabla v\|^2; \tag{1.3}$$

see [28, Lemma 2] for the proof that $c_0 \leqslant 1/\pi$ as well as for uniqueness results for $1 < p \leqslant 3$.

We refer to the monographs [21] and [10] and to the review articles [15] and [11] for structure-preserving numerical methods for ordinary differential equations (o.d.e's) as well as for partial differential equations. An important advantage of structure-preserving methods is that they exhibit improved long time behavior; cf., e.g., [18], for the NLS equation. In the case of the NLS equation, particularly desirable properties of numerical methods are the conservation of the mass (density) and energy at the discrete level.

A popular structure-preserving modified Crank–Nicolson scheme for (1.1), widely used in computations in finite difference or finite element contexts, was introduced by Delfour, Fortin, and Payre, [17]; see (3.8); the differencing of the nonlinear term is motivated by a method of Strauss and Vazquez, [37], for the Klein–Gordon equation. We briefly discuss this method in section 3. So-called *relaxation*, second order methods, introduced in [6,7] for the cubic NLS equation and in [8] for higher power nonlinearities, are L^2-conservative

and preserve a modified discrete energy. These methods are *linearly implicit* for the cubic NLS equation and nonlinear for higher power nonlinearities. In [8] and [42] second order convergence for the cubic NLS equation and for general nonlinearities, respectively, is established. A second order two-step scheme for the original form of the NLS equation satisfying discrete analogues at two consecutive time levels of the mass (density) and energy conservations was proposed and implemented in [19]; this method is analyzed in [41] and [42]. High-order energy-preserving methods for the one-dimensional NLS equation are considered in [5] and [12].

For exponential integrators for the NLS equation, we refer to [25, 13, 14, 16] and references therein; notice that the projected explicit Lawson methods of [13] preserve the L^2-norm and the momentum, rather than the energy, for special initial values. In [14] schemes with exact conservation of the discrete L^2-norm and/or energy are constructed by projection and/or design of the schemes. See [22, pp. 472–474] for the basic idea for projection methods for o.d.e's with invariants. For numerical methods that nearly conserve mass, energy and momentum over long times, see [16].

The outline of this paper is as follows. In Section 2 we present the SAV reformulation of the NLS equation; see (2.13). In Section 3 we briefly recall the L^2-conservative standard Crank–Nicolson method as well as the L^2- and energy-conservative modified Crank–Nicolson method. We also note that the continuous Galerkin methods are energy-preserving.

In contrast to the standard formulation (1.1), as we shall see in Section 4, the SAV–Gauss methods, i.e., the Gauss methods for the SAV reformulation (2.13) of the NLS equation, are L^2-conservative and satisfy the analogue of the energy conservation property (2.8) at the discrete level. For the convenience of the reader, we treat the one-stage (midpoint) Gauss method, i.e., the Crank–Nicolson method, first and subsequently the general case. Numerical results are presented in Section 5.

2 The SAV reformulation of the NLS equation

In this section we present the SAV reformulation of the NLS equation. For the sake of completeness, we give also details of the derivation of the well-known invariance properties (1.2).

We denote by $(\cdot,\cdot)$ and $\|\cdot\|$ the L^2 inner product and the corresponding norm, and by $\|\cdot\|_{L^q}$ the L^q-norm.

2.1 Invariants

Testing the NLS equation in (1.1) against u and against u_t, respectively, and integrating by parts in the first term on the right-hand side, we have

$$\frac{1}{2}\frac{d}{dt}\|u(\cdot,t)\|^2 + \mathrm{i}\,\mathrm{Im}(u_t(\cdot,t),u(\cdot,t)) = -\mathrm{i}\|\nabla u(\cdot,t)\|^2 + \mathrm{i}\lambda\|u(\cdot,t)\|_{L^{p+1}}^{p+1} \tag{2.1}$$

and

$$\begin{aligned}\|u_t(\cdot,t)\|^2 = {}& \mathrm{Im}(\nabla u,\nabla u_t) - \lambda\left(|u(\cdot,t)|^{p-1},\mathrm{Im}(u(\cdot,t)\overline{u_t(\cdot,t)})\right)\\ & -\mathrm{i}\frac{1}{2}\frac{d}{dt}\Big(\|\nabla u(\cdot,t)\|^2 - \frac{2\lambda}{p+1}\|u(\cdot,t)\|_{L^{p+1}}^{p+1}\Big),\end{aligned} \tag{2.2}$$

$0 < t \leqslant T$, respectively. Notice that in the derivation of (2.2) the simple calculation

$$\partial_t \big(|u(x,t)|^{p+1}\big) = (p+1)|u(x,t)|^{p-1}\,\mathrm{Re}\,\big(u(x,t)\overline{u_t(x,t)}\big) \tag{2.3}$$

is used. Taking real and imaginary parts in (2.1) and (2.2), respectively, we see that both the L^2-norm (charge, density, mass) and the energy (Hamiltonian) $E(u(\cdot,t))$ are conserved,

$$\|u(\cdot,t)\| = \|u^0\|, \quad 0 \leqslant t \leqslant T, \tag{2.4}$$

and

$$E(u(\cdot,t)) = \|\nabla u(\cdot,t)\|^2 - \frac{2\lambda}{p+1}\|u(\cdot,t)\|_{L^{p+1}}^{p+1} = E(u^0), \quad 0 \leqslant t \leqslant T, \tag{2.5}$$

respectively. The Hamiltonian plays a more important role in the case of the *defocusing* NLS, i.e., for negative λ, than in the case of the *focusing* NLS, i.e., for positive λ.

2.2 The SAV approach

The scalar auxiliary variable (SAV) approach, motivated by the invariant energy quadratization (IEQ) technique of [39] and [40], was introduced in [33] and [34] for gradient flows. In both approaches, the energy is expressed in terms of Hilbert space norms of the new variables; this fact considerably simplifies the construction of structure-preserving numerical methods. We could have also used the IEQ approach here; we have chosen the SAV approach since, in contrast to the IEQ approach, it only slightly increases the computational cost.

We introduce the scalar real-valued function r,

$$r(t) := \Big(\frac{1}{p+1}\|u(\cdot,t)\|_{L^{p+1}}^{p+1}\Big)^{1/2} = \frac{1}{\sqrt{p+1}}\|u(\cdot,t)\|_{L^{p+1}}^{\frac{p+1}{2}}, \quad 0 \leqslant t \leqslant T, \tag{2.6}$$

and let $W(\upsilon)$ be given by

$$W(\upsilon) := \frac{|\upsilon|^{p-1}\upsilon}{\Big(\frac{1}{p+1}\|\upsilon\|_{L^{p+1}}^{p+1}\Big)^{1/2}}. \tag{2.7}$$

In view of (2.6), the energy is expressed as

$$E(u(\cdot,t)) = \|\nabla u(\cdot,t)\|^2 - 2\lambda|r(t)|^2,$$

and the energy conservation property (2.5) can be written in the form

$$\|\nabla u(\cdot,t)\|^2 - 2\lambda|r(t)|^2 = \|\nabla u^0\|^2 - 2\lambda|r^0|^2, \quad 0 \leqslant t \leqslant T, \tag{2.8}$$

with $r^0 := r(0)$. Notice that the energy is expressed in terms of Hilbert space norms of the new variables; this is the main advantage of the SAV approach for the NLS equation.

Then, obviously, the NLS equation can be written in the form

$$u_t = \mathrm{i}\Delta u + \mathrm{i}\lambda r W(u) \quad \text{in } \Omega \times (0,T]. \tag{2.9}$$

Now,

$$r'(t) = \frac{1}{2(p+1)} \frac{1}{\left(\frac{1}{p+1}\|u(\cdot,t)\|_{L^{p+1}}^{p+1}\right)^{1/2}} \left(\|u(\cdot,t)\|_{L^{p+1}}^{p+1}\right)'. \tag{2.10}$$

Consider now the last factor on the right-hand side of (2.10). We have

$$\left(\|u(\cdot,t)\|_{L^{p+1}}^{p+1}\right)' = \frac{d}{dt}\int_\Omega |u(x,t)|^{p+1}\,\mathrm{d}x,$$

whence

$$\left(\|u(\cdot,t)\|_{L^{p+1}}^{p+1}\right)' = \int_\Omega \partial_t\left(|u(x,t)|^{p+1}\right)\mathrm{d}x. \tag{2.11}$$

Substituting (2.3) into (2.11) and the result into (2.10), we obtain

$$r'(t) = \frac{1}{2}\mathrm{Re}(W(u),u_t), \quad 0 \leqslant t \leqslant T. \tag{2.12}$$

Summarizing, the SAV reformulation of the initial and boundary value problem (1.1) is

$$\begin{cases} u_t = \mathrm{i}\Delta u + \mathrm{i}\lambda r W(u) & \text{in } \Omega\times[0,T], \\ u = 0 & \text{on } \partial\Omega\times[0,T], \\ r'(t) = \dfrac{1}{2}\mathrm{Re}(W(u),u_t) & \text{in } [0,T], \\ u(\cdot,0) = u^0 & \text{in } \bar{\Omega}, \\ r(0) = \dfrac{1}{\sqrt{p+1}}\|u^0\|_{L^{p+1}}^{\frac{p+1}{2}}. \end{cases} \tag{2.13}$$

Remark 2.1 (Definition of r and W) Notice that, in view of (2.4), for $u^0 \neq 0$, $W(u(\cdot,t))$ is well defined for all $t \in [0,T]$; the case $u^0 = 0$ is not of interest, since the solution u vanishes for all t. We could, however, have added a positive constant c in the expression in the square roots in the definition of r and in the denominator of W.

Remark 2.2 (General form of the NLS equation) We replace the power nonlinearity in the NLS equation in (1.1) by a general nonlinearity, and consider the corresponding initial and boundary value problem for the general NLS equation

$$u_t = \mathrm{i}\Delta u + \mathrm{i}f(u) \tag{2.14}$$

with $f(v) := g(|v|^2)v$ and g a continuous real-valued function. Let G be such that $G' = g$ and $G(0) = 0$, and let $F(v) := \frac{1}{2}G(|v|^2)$ be bounded from below.

Testing (2.14) against u and against u_t, respectively, and integrating by parts in the first term on the right-hand side, we have, in analogy to (2.1) and (2.2),

$$\frac{1}{2}\frac{d}{dt}\|u(\cdot,t)\|^2 + \mathrm{i}\,\mathrm{Im}(u_t(\cdot,t),u(\cdot,t)) = -\mathrm{i}\|\nabla u(\cdot,t)\|^2 + \mathrm{i}\left(g(|u|^2),|u|^2\right) \tag{2.15}$$

and

$$\begin{aligned} \|u_t(\cdot,t)\|^2 = {} & \mathrm{Im}(\nabla u,\nabla u_t) - \left(g(|u(\cdot,t)|^2),\mathrm{Im}(u(\cdot,t)\overline{u_t(\cdot,t)})\right) \\ & -\mathrm{i}\frac{d}{dt}\left(\frac{1}{2}\|\nabla u(\cdot,t)\|^2 - \int_\Omega F\left(u(x,t)\right)\mathrm{d}x\right), \end{aligned} \tag{2.16}$$

$0 \leqslant t \leqslant T$, respectively. In the derivation of (2.16) we used the easy calculation

$$\partial_t F\big(u(x,t)\big) = g(|u(x,t)|^2)\,\mathrm{Re}(u(x,t)\overline{u_t(x,t)}). \tag{2.17}$$

Taking real and imaginary parts in (2.15) and (2.16), respectively, we see that both the L^2-norm and the energy $E(u(\cdot,t))$ are conserved,

$$\|u(\cdot,t)\| = \|u^0\|, \quad 0 \leqslant t \leqslant T, \tag{2.18}$$

and

$$E(u(\cdot,t)) := \frac{1}{2}\|\nabla u(\cdot,t)\|^2 - \int_\Omega F\big(u(x,t)\big)\,\mathrm{d}x = E(u^0), \quad 0 \leqslant t \leqslant T, \tag{2.19}$$

respectively.

The NLS equation in (1.1) is a special case of (2.14) with $g(\upsilon) := \lambda\,\upsilon^{\frac{p-1}{2}}$. The results of this paper can be easily extended to the general NLS equation (2.14).

The Fréchet derivative E' of the energy functional $E(u)$ of (2.19) is $E'(u) = -\Delta u - f(u)$; therefore, the NLS equation (2.14) can be written in Hamiltonian form,

$$u_t = -\mathrm{i}E'(u); \tag{2.20}$$

notice that the multiplication by $-\mathrm{i}$ is a skew operator. This explains why the energy $E(u)$ is also referred to as *the Hamiltonian* of the NLS equation (2.14). Because

$$\frac{d}{dt}E(u) = \big(E'(u), u_t\big) = \mathrm{i}\big(E'(u), E'(u)\big)$$

and the quantity on the left-hand side is real, the Hamiltonian form (2.20) immediately yields that the energy $E(u)$ is a constant.

For completeness, let us derive the SAV reformulation of the general form of the NLS equation. Let c be such that $F + c|\Omega|$ is strictly positive.

We introduce the positive function r,

$$r(t) := \Big(\int_\Omega F\big(u(x,t)\big)\,\mathrm{d}x + c\Big)^{1/2}, \quad 0 \leqslant t \leqslant T, \tag{2.21}$$

and let $W(\upsilon)$ be given by

$$W(\upsilon) := \frac{g(|\upsilon|^2)\upsilon}{\big(\int_\Omega F(\upsilon)\,\mathrm{d}x + c\big)^{1/2}}. \tag{2.22}$$

In view of (2.17), we have

$$r'(t) = \frac{1}{2}\mathrm{Re}(W(u), u_t), \quad 0 \leqslant t \leqslant T. \tag{2.23}$$

Summarizing, the SAV reformulation of the initial and boundary value problem for the general NLS equation (2.14) is

$$\begin{cases} u_t = \mathrm{i}\Delta u + \mathrm{i}rW(u) & \text{in } \Omega \times [0,T], \\ u = 0 & \text{on } \partial\Omega \times [0,T], \\ r'(t) = \dfrac{1}{2}\mathrm{Re}(W(u), u_t) & \text{in } [0,T], \\ u(\cdot,0) = u^0 & \text{in } \bar{\Omega}, \\ r(0) = \Big(\displaystyle\int_\Omega F\big(u^0(x)\big)\,\mathrm{d}x + c\Big)^{1/2}. \end{cases} \tag{2.24}$$

3 Crank–Nicolson methods for (1.1)

For the convenience of the reader, in this section we recall the standard as well as the modified Crank–Nicolson methods for (1.1) and their well-known conservation properties.

Let $N \in \mathbb{N}$ and, for simplicity, consider a uniform partition $t_n := n\tau, n = 0, \dots, N$, of the time interval $[0,T]$ with time step $\tau := T/N$. For a given sequence $v^n, n = 0, \dots, N$, we denote by $\bar\partial v^{n+1}$ and by $v^{n+\frac12}$ the backward difference quotient and the average, respectively,

$$\bar\partial v^{n+1} := \frac{v^{n+1} - v^n}{\tau}, \quad v^{n+\frac12} := \frac{v^{n+1} + v^n}{2}, \quad n = 0, \dots, N-1.$$

The standard Crank–Nicolson method. With starting value $U^0 := u^0$, the Crank–Nicolson approximations $U^\ell \in H^1_0(\Omega)$ to the nodal values $u(\cdot, t_\ell)$ of the solution u of the initial and boundary value problem (1.1), are recursively defined by

$$\bar\partial U^{n+1} = \mathrm{i}\Delta U^{n+\frac12} + \mathrm{i}\lambda |U^{n+\frac12}|^{p-1} U^{n+\frac12}, \quad n = 0, \dots, N-1. \tag{3.1}$$

It is easily seen that the Crank–Nicolson method is L^2-conservative but not energy-conservative. Indeed, testing (3.1) against $U^{n+\frac12}$ and integrating by parts in the first term on the right-hand side, we have

$$(\bar\partial U^{n+1}, U^{n+\frac12}) = -\mathrm{i}\|\nabla U^{n+\frac12}\|^2 + \mathrm{i}\lambda \|U^{n+\frac12}\|^{p+1}_{L^{p+1}(\Omega)},$$

and thus, since the right-hand side is imaginary,

$$\mathrm{Re}(\bar\partial U^{n+1}, U^{n+\frac12}) = 0.$$

Now, $\mathrm{Re}(\bar\partial U^{n+1}, U^{n+\frac12}) = \frac{1}{2\tau}\big[\|U^{n+1}\|^2 - \|U^n\|^2\big]$, and we obtain the invariance property

$$\|U^{n+1}\| = \|U^n\|, \quad n = 0, \dots, N-1, \tag{3.2}$$

a discrete analogue of (2.4).

Furthermore, testing (3.1) against $\bar\partial U^{n+1}$ and integrating by parts in the first term on the right-hand side, we have

$$\|\bar\partial U^{n+1}\|^2 = -\mathrm{i}(\nabla U^{n+\frac12}, \nabla \bar\partial U^{n+1}) + \mathrm{i}\lambda \big(|U^{n+\frac12}|^{p-1} U^{n+\frac12}, \bar\partial U^{n+1}\big). \tag{3.3}$$

Taking imaginary parts in (3.3), we obtain

$$\|\nabla U^{n+1}\|^2 - \lambda \int_\Omega |U^{n+\frac12}|^{p-1} |U^{n+1}|^2 \,\mathrm{d}x = \|\nabla U^n\|^2 - \lambda \int_\Omega |U^{n+\frac12}|^{p-1} |U^n|^2 \,\mathrm{d}x, \tag{3.4}$$

i.e.,

$$E(U^{n+1}) = E(U^n) + \lambda \mathscr{D}(U^n, U^{n+1}), \quad n = 0, \dots, N-1, \tag{3.5}$$

with the discrepancy term $\mathscr{D}(U^n, U^{n+1})$,

$$\mathscr{D}(U^n, U^{n+1}) := \int_\Omega \Big[\frac{2}{p+1}\big(|U^{n+1}|^{p+1} - |U^n|^{p+1}\big) - |U^{n+\frac12}|^{p-1}\big(|U^{n+1}|^2 - |U^n|^2\big)\Big] \,\mathrm{d}x. \tag{3.6}$$

The discrepancy term $\mathscr{D}(U^n,U^{n+1})$ does not vanish, in general; therefore, the standard Crank–Nicolson method for (1.1) is *not* energy-conservative.

A structure-preserving modified Crank–Nicolson method. Motivated by the form (3.6) of the discrepancy term $\mathscr{D}(U^n,U^{n+1})$, we modify the Crank–Nicolson method (3.1) by replacing $|U^{n+\frac12}|^{p-1}$ by

$$\frac{2}{p+1}\frac{|U^{n+1}|^{p+1}-|U^n|^{p+1}}{|U^{n+1}|^2-|U^n|^2}, \quad 1<p<\infty, \tag{3.7}$$

i.e., we consider the method, cf. [17],

$$\bar\partial U^{n+1}=\mathrm{i}\Delta U^{n+\frac12}+\mathrm{i}\lambda\frac{2}{p+1}\frac{|U^{n+1}|^{p+1}-|U^n|^{p+1}}{|U^{n+1}|^2-|U^n|^2}U^{n+\frac12}, \quad n=0,\dots,N-1. \tag{3.8}$$

The expression (3.7) takes simpler forms for odd p; of course, for the cubic NLS, $p=3$, it reduces to $\big(|U^{n+1}|^2+|U^n|^2\big)/2$.

Since the inner product of the last term on the right-hand side of (3.8) with $U^{n+\frac12}$ is imaginary, the second-order method (3.8) is L^2-conservative, it satisfies

$$\|U^{n+1}\|=\|U^n\|, \quad n=0,\dots,N-1. \tag{3.9}$$

Furthermore, it is easily seen that it also satisfies

$$E(U^{n+1})=E(U^n), \quad n=0,\dots,N-1, \tag{3.10}$$

i.e., the method is energy-conservative.

In the case of the general NLS equation, the analogue to (3.8) structure-preserving modified Crank–Nicolson method is

$$\bar\partial U^{n+1}=\mathrm{i}\Delta U^{n+\frac12}+2\mathrm{i}\frac{F(U^{n+1})-F(U^n)}{|U^{n+1}|^2-|U^n|^2}U^{n+\frac12}, \quad n=0,\dots,N-1. \tag{3.11}$$

Remark 3.1 (Energy-preservation of the continuous Galerkin method) Let $I_n:=(t_n,t_{n+1}]$ and $q\in\mathbb{N}$. To formulate the *continuous Galerkin* method for (1.1), we let the space $\mathscr{V}_q^c$ consist of continuous functions in time that are piecewise polynomials of degree at most q in each I_n, with coefficients in the Sobolev space $V=H_0^1(\Omega)$ of complex-valued functions on Ω, i.e.,

$$\mathscr{V}_q^c:=\{\varphi\in C([0,T];V):\varphi|_{I_n}(t)=\sum_{j=0}^q \upsilon_j t^j,\ n=0,\dots,N-1\}.$$

The time discrete continuous Galerkin approximation U to the solution u of (1.1) is defined as follows: We seek $U\in\mathscr{V}_q^c$ such that $U(\cdot,0)=u(\cdot,0)$ and

$$\int_{I_n}[(U_t,\upsilon)+\mathrm{i}(\nabla U,\nabla\upsilon)-\mathrm{i}\lambda(|U|^{p-1}U,\upsilon)]\,\mathrm{d}t=0 \quad \forall\upsilon\in\mathscr{V}_{q-1}(I_n), \tag{3.12}$$

for $n=0,\dots,N-1$. Here $\mathscr{V}_s(I_n):=\{\varphi|_{I_n}:\varphi\in\mathscr{V}_s^c\}$.

Since $U_t\in\mathscr{V}_{q-1}(I_n)$, choosing the test function $\upsilon=U_t$ in (3.12) and taking imaginary parts, we easily see, as in the continuous case, cf. the derivation of (2.5), that

$$\int_{I_n}\frac{d}{dt}E\big(U(\cdot,t)\big)\,\mathrm{d}t=0 \tag{3.13}$$

and infer that $E\big(U(\cdot,t_{n+1})\big) = E\big(U(\cdot,t_n)\big)$. This shows that the continuous Galerkin method preserves the energy at the *nodes* of the partition,

$$E\big(U(\cdot,t_n)\big) = E(u^0), \quad n = 1,\dots,N. \tag{3.14}$$

Notice, however, that the continuous Galerkin method is *not* L^2-conservative. This is due to the fact that $U \in \mathscr{V}_q(I_n)$ is, in general, not an element of $\mathscr{V}_{q-1}(I_n)$, whence it cannot be used as a test function in the continuous Galerkin method (3.12). We refer to [24] for the analysis of the continuous Galerkin method for the cubic NLS equation.

4 SAV–Gauss methods

In this section, we construct the SAV–Gauss methods, applying the Gauss methods to the SAV reformulation (2.13) of the NLS equation, and show that they are L^2-conservative and satisfy a discrete analogue of the energy conservation property (2.8); cf. (4.10) and (4.11). We also discuss some computationally advantageous linearizations of the SAV–Gauss methods and their conservation properties.

For the reader's convenience, we first consider the second order SAV–Crank–Nicolson method and subsequently high order SAV–Gauss methods.

4.1 SAV–Crank–Nicolson method

With starting values $U^0 := u^0$ and $R^0 := r(0)$, we consider the SAV–Crank–Nicolson approximations $U^\ell \in H_0^1(\Omega)$ and $R^\ell \in \mathbb{R}$ to the nodal values $u(\cdot,t_\ell)$ and $r(t_\ell)$ of the solutions u and r of the initial and boundary value problem (2.13), defined recursively by

$$\begin{cases} \bar\partial U^{n+1} = \mathrm{i}\Delta U^{n+\frac12} + \mathrm{i}\lambda R^{n+\frac12} W(U^{n+\frac12}), \\ \bar\partial R^{n+1} = \dfrac{1}{2}\,\mathrm{Re}\,\big(W(U^{n+\frac12}), \bar\partial U^{n+1}\big), \end{cases} \qquad n = 0,\dots,N-1. \tag{4.1}$$

Motivated by the energy conservation property (2.8), we denote by $E_\tau(U^n,R^n)$,

$$E_\tau(U^n,R^n) := \|\nabla U^n\|^2 - 2\lambda |R^n|^2,$$

the discrete energy (also referred to as modified energy since, in general, $|R^n|^2$ does not coincide with $\frac{1}{p+1}\|U^n\|^{p+1}_{L^{p+1}(\Omega)}$) of the numerical solution at t_n.

Lemma 4.1 (Structure preservation of the SAV–Crank–Nicolson method) *The SAV–Crank–Nicolson method* (4.1) *is L^2-conservative and satisfies a discrete analogue of* (2.8)*, namely*

$$\|U^{n+1}\| = \|U^n\|, \quad n = 0,\dots,N-1, \tag{4.2}$$

as well as

$$E_\tau(U^{n+1},R^{n+1}) = E_\tau(U^n,R^n), \quad n = 0,\dots,N-1. \tag{4.3}$$

Proof Testing the first equation of (4.1) against $\bar\partial U^{n+1}$ and integrating by parts in the first term on the right-hand side, we have

$$\|\bar\partial U^{n+1}\|^2 = -\mathrm{i}(\nabla U^{n+\frac12},\nabla\bar\partial U^{n+1}) + \mathrm{i}\lambda R^{n+\frac12}\big(W(U^{n+\frac12}),\bar\partial U^{n+1}\big). \tag{4.4}$$

Now,

$$\begin{aligned}(\nabla U^{n+\frac12},\nabla\bar\partial U^{n+1}) &= \frac{1}{2\tau}(\nabla U^{n+1}+\nabla U^n,\nabla U^{n+1}-\nabla U^n)\\ &= \frac{1}{2\tau}\Big\{\big[\|\nabla U^{n+1}\|^2-\|\nabla U^n\|^2\big]+\big[(\nabla U^n,\nabla U^{n+1})-(\nabla U^{n+1},\nabla U^n)\big]\Big\};\end{aligned}$$

the last term is imaginary and we see that

$$\mathrm{Re}(\nabla U^{n+\frac12},\nabla\bar\partial U^{n+1}) = \frac{1}{2\tau}\big[\|\nabla U^{n+1}\|^2-\|\nabla U^n\|^2\big] = \frac12\bar\partial\|\nabla U^{n+1}\|^2. \tag{4.5}$$

Therefore, taking imaginary parts in (4.4), we obtain

$$-\frac12\bar\partial\|\nabla U^{n+1}\|^2 + \lambda R^{n+\frac12}\,\mathrm{Re}(W(U^{n+\frac12}),\bar\partial U^{n+1}) = 0. \tag{4.6}$$

Using here the second equation of (4.1), we have

$$-\frac12\bar\partial\|\nabla U^{n+1}\|^2 + 2\lambda R^{n+\frac12}\bar\partial R^{n+1} = 0,$$

i.e.,

$$-\frac12\bar\partial\|\nabla U^{n+1}\|^2 + 2\lambda\frac{1}{2\tau}\big(|R^{n+1}|^2-|R^n|^2\big) = 0,$$

whence

$$\bar\partial\|\nabla U^{n+1}\|^2 - 2\lambda\bar\partial|R^{n+1}|^2 = 0,$$

and see that the energy conservation property (4.3) holds true. Notice that, since $|R^n|$ does not coincide with $\frac{1}{\sqrt{p+1}}\|U^n\|^{\frac{p+1}{2}}_{L^{p+1}(\Omega)}$, in general, (4.3) is the discrete analogue of (2.8) and a modified discrete analogue of (2.5).

Testing the first equation of (4.1) against $U^{n+\frac12}$ and integrating by parts in the first term on the right-hand side, we have

$$(\bar\partial U^{n+1},U^{n+\frac12}) = -\mathrm{i}\|\nabla U^{n+\frac12}\|^2 + \mathrm{i}\lambda R^{n+\frac12}\big(W(U^{n+\frac12}),U^{n+\frac12}\big),$$

and thus, since the right-hand side is imaginary,

$$\mathrm{Re}(\bar\partial U^{n+1},U^{n+\frac12}) = 0;$$

as in Section 3, we infer that (4.2) is valid. The discrete invariance property (4.2) is the discrete analogue of (2.4). Notice that, in the derivation of (4.2), from the second equation of (4.1) we only used the fact that $R^{n+\frac12}$ is real. □

4.2 High order SAV–Gauss methods

Here, we construct the SAV–Gauss methods, applying the Gauss methods to the SAV reformulation (2.13) of the NLS equation, and show that they are L^2-conservative and satisfy a discrete analogue of the energy conservation property (2.8); cf. (4.10) and (4.11). We also discuss some computationally advantageous linearizations of the SAV–Gauss methods and their conservation properties.

For $q \in \mathbb{N}$, the q-stage Gauss method is specified by the Gauss points $0 < c_1 < \cdots < c_q < 1$ in $[0,1]$, i.e., the roots of the shifted Legendre polynomial of degree q, and the coefficients a_{ij} and b_i such that the *stage order* of the method be q, i.e., satisfying the following conditions:

$$\text{(B}(q)\text{)} \qquad \sum_{i=1}^{q} b_i c_i^{\ell-1} = \frac{1}{\ell}, \qquad \ell = 1,\dots,q,$$

$$\text{(C}(q)\text{)} \qquad \sum_{j=1}^{q} a_{ij} c_j^{\ell-1} = \frac{c_i^{\ell}}{\ell}, \quad \ell = 1,\dots,q,\ i = 1,\dots,q.$$

It is well known that the first relation, (B(q)), is actually valid for $\ell = 1,\dots,2q$; the q-stage Gauss method is the only q-stage Runge–Kutta method of the highest possible order $p, p = 2q$. The matrix $A = (a_{ij})_{i,j=1,\dots,q}$ is obviously invertible.

It is, furthermore, well known that the weights $b_1,\dots,b_q$ are positive and that the $q \times q$ symmetric matrix M with entries $m_{ij} := b_i a_{ij} + b_j a_{ji} - b_i b_j, i, j = 1,\dots,q$, vanishes. In particular, the Gauss methods are *algebraically stable*. See, e.g., [22, §IV.5, §IV.12].

The first member of this family, for $q = 1$, is the (implicit) midpoint method, i.e., the Crank–Nicolson method. Since this method is symplectic, it conserves quadratic invariants; see, e.g., [32].

Assuming that nodal approximations U^n, R^n to the nodal values $u(\cdot,t_n)$ and $r(t_n)$, respectively, have been computed, to include the study of possible linearizations and to avoid repetitions, we consider the following variant of the q-stage Gauss method for the SAV reformulation (2.13) of the initial and boundary value problem (1.1):

$$\text{(4.7)} \qquad \begin{cases} \dot{U}^{ni} = \mathrm{i}\Delta U^{ni} + \mathrm{i}\lambda R^{ni} W(\widetilde{U}^{ni}) & \text{in } \Omega, \quad i = 1,\dots,q, \\ U^{ni} = U^n + \tau \sum_{j=1}^{q} a_{ij} \dot{U}^{nj} & \text{in } \Omega, \quad i = 1,\dots,q, \\ U^{ni} = 0 & \text{on } \partial\Omega, \quad i = 1,\dots,q, \end{cases}$$

$$\text{(4.8)} \qquad \begin{cases} \dot{R}^{ni} = \dfrac{1}{2} \mathrm{Re}(W(\widetilde{U}^{ni}), \dot{U}^{ni}), & i = 1,\dots,q, \\ R^{ni} = R^n + \tau \sum_{j=1}^{q} a_{ij} \dot{R}^{nj}, & i = 1,\dots,q; \end{cases}$$

in Remark 4.1 we discuss three interesting choices for $\widetilde{U}^{ni}$. Note that the quantities $\dot{U}^{ni}$ and $\dot{R}^{ni}$ have been introduced here for notational convenience only. In fact, substituting $\dot{U}^{ni}$ from the first relation of (4.7) into the second relation of (4.7) as well as into the first relation of (4.8), and subsequently substituting the new first relation of (4.8) into its second relation, we obtain a coupled system for the internal stages U^{ni} and R^{ni}, $i = 1,\dots,q$. In case the quantities $\widetilde{U}^{ni}$ are known, the implementation of (4.7)–(4.8) requires only the solution of a

coupled linear system for $(U^{ni},R^{ni}) \in H_0^1(\Omega)\times\mathbb{R}$, $i=1,\dots,q$. Once U^{ni} and R^{ni} have been determined, we obtain the quantities $\dot{U}^{ni} \in H_0^1(\Omega)$ and $\dot{R}^{ni} \in \mathbb{R}$ from the second relations of (4.7) and (4.8), respectively, using the invertibility of the matrix $A=(a_{ij})$. Using these values, one computes the new approximations $(U^{n+1},R^{n+1}) \in H_0^1(\Omega)\times\mathbb{R}$ at the next time level t_{n+1} through

$$\begin{cases} U^{n+1} := U^n + \tau \sum_{i=1}^{q} b_i \dot{U}^{ni}, \\ R^{n+1} := R^n + \tau \sum_{i=1}^{q} b_i \dot{R}^{ni}. \end{cases} \tag{4.9}$$

Remark 4.1 (Some choices for $\widetilde{U}^{ni}$) Let $\widetilde{U}^{ni} := U^{ni}, i=1,\dots,q$, with unknown internal stages U^{ni}. Then, the scheme (4.7)–(4.9) reduces to the base (nonlinear) SAV–Gauss method; for a detailed analysis of Gauss methods applied to the original initial and boundary value problem (1.1), we refer to [23].

Next, consider the fixed-point linearization of the SAV–Gauss method, i.e., with given $\widetilde{U}^{ni} = U^{ni}_{\ell-1}$ and unknown $U^{ni} = U^{ni}_{\ell}$; see [3] for an analysis of this variant applied to the original initial and boundary value problem (1.1).

A third possibility is to define $\widetilde{U}^{ni}$ by polynomial extrapolation of the values of the intermediate approximations at the preceding time interval; see [4] for the case of the Allen–Cahn equation and [26] for the case of the wave equation.

Theorem 4.1 (Structure preservation of the SAV–Gauss methods) *The SAV–Gauss method, i.e., the method* (4.7)–(4.9) *with $\widetilde{U}^{ni} = U^{ni}, i=1,\dots,q$, is L^2-conservative and satisfies a discrete analogue of* (2.8)*, namely*

$$\|U^{n+1}\| = \|U^n\|, \quad n=0,\dots,N-1, \tag{4.10}$$

as well as

$$E_\tau(U^{n+1},R^{n+1}) = E_\tau(U^n,R^n), \quad n=0,\dots,N-1. \tag{4.11}$$

Proof According to the first relation of (4.9), we have

$$\nabla U^{n+1} = \nabla U^n + \tau \sum_{i=1}^{q} b_i \nabla \dot{U}^{ni}.$$

Squaring the L^2-norms of both sides, i.e., taking the inner product of each side by itself, we obtain

$$\begin{aligned} \|\nabla U^{n+1}\|^2 &= \Big(\nabla U^n + \tau \sum_{i=1}^{q} b_i \nabla \dot{U}^{ni}, \nabla U^n + \tau \sum_{j=1}^{q} b_j \nabla \dot{U}^{nj}\Big) \\ &= \|\nabla U^n\|^2 + \tau \sum_{i=1}^{q} b_i \big[(\nabla \dot{U}^{ni}, \nabla U^n) + (\nabla U^n, \nabla \dot{U}^{ni})\big] + \tau^2 \sum_{i,j=1}^{q} b_i b_j (\nabla \dot{U}^{ni}, \nabla \dot{U}^{nj}). \end{aligned}$$

Substituting $U^n = U^{ni} - \tau \sum_{j=1}^{q} a_{ij} \dot{U}^{nj}$ (the second relation in (4.7)) into the second term on the right-hand side of the last relation, we obtain

$$\|\nabla U^{n+1}\|^2 = \|\nabla U^n\|^2 + 2\tau \sum_{i=1}^{q} b_i \operatorname{Re}\big(\nabla \dot{U}^{ni}, \nabla U^{ni}\big) - \tau^2 \sum_{i,j=1}^{q} m_{ij} (\nabla \dot{U}^{ni}, \nabla \dot{U}^{nj}),$$

whence

$$\|\nabla U^{n+1}\|^2 = \|\nabla U^n\|^2 + 2\tau \sum_{i=1}^{q} b_i \,\mathrm{Re}\,(\nabla \dot{U}^{ni}, \nabla U^{ni}), \tag{4.12}$$

since $m_{ij} = 0, i, j = 1, \ldots, q$. Testing the first relation of (4.7) by $\dot{U}^{ni}$ yields

$$\|\dot{U}^{ni}\|^2 = -\mathrm{i}(\nabla U^{ni}, \nabla \dot{U}^{ni}) + \mathrm{i}\lambda R^{ni}(W(\widetilde{U}^{ni}), \dot{U}^{ni}),$$

which implies $\mathrm{Re}(\nabla \dot{U}^{ni}, \nabla U^{ni}) = \lambda R^{ni}\,\mathrm{Re}(W(\widetilde{U}^{ni}), \dot{U}^{ni})$. Then, substituting this into (4.12), we get

$$\|\nabla U^{n+1}\|^2 = \|\nabla U^n\|^2 + 2\lambda\tau \sum_{i=1}^{q} b_i R^{ni}\,\mathrm{Re}(W(\widetilde{U}^{ni}), \dot{U}^{ni}). \tag{4.13}$$

Using here the first relation of (4.8), we obtain

$$\|\nabla U^{n+1}\|^2 = \|\nabla U^n\|^2 + 4\lambda\tau \sum_{i=1}^{q} b_i \dot{R}^{ni} R^{ni}. \tag{4.14}$$

Similarly, we can obtain

$$|R^{n+1}|^2 = |R^n|^2 + 2\tau \sum_{i=1}^{q} b_i \dot{R}^{ni} R^{ni} - \tau^2 \sum_{i,j=1}^{q} m_{ij} \dot{R}^{ni} \dot{R}^{nj},$$

i.e.,

$$|R^{n+1}|^2 = |R^n|^2 + 2\tau \sum_{i=1}^{q} b_i \dot{R}^{ni} R^{ni}. \tag{4.15}$$

Notice that up to this point we followed the proof for the algebraic stability of the Gauss methods; since we are interested in the energy conservation property, we do not consider differences of approximations.

Now, multiplying (4.15) by 2λ and subtracting the result from (4.14), the last terms on their right-hand sides cancel and we obtain the discrete energy invariance property (4.11).

The Gauss methods applied to (1.1) are L^2-conservative; see [23,2]. As we shall see, this is the case also for the (nonlinear) SAV–Gauss methods, applied to (2.13).

Indeed, squaring the L^2-norms of both sides of the first relation in (4.9), i.e., taking the L^2-inner products of both sides by themselfs, we obtain

$$\|U^{n+1}\|^2 = \|U^n\|^2 + \tau \sum_{i=1}^{q} b_i \big[(\dot{U}^{ni}, U^n) + (U^n, \dot{U}^{ni})\big] + \tau^2 \sum_{i,j=1}^{q} b_i b_j (\dot{U}^{ni}, \dot{U}^{nj}).$$

Replacing U^n in the second term on the right-hand side by $U^{ni} - \tau \sum_{j=1}^{q} a_{ij} \dot{U}^{nj}$, see the second relation in (4.7), we have

$$\|U^{n+1}\|^2 = \|U^n\|^2 + \tau \sum_{i=1}^{q} b_i \big[(\dot{U}^{ni}, U^{n,i}) + (U^{n,i}, \dot{U}^{ni})\big] - \tau^2 \sum_{i,j=1}^{q} m_{ij} (\dot{U}^{ni}, \dot{U}^{nj}).$$

As already noted, $m_{ij} = 0$, and thus

$$\|U^{n+1}\|^2 = \|U^n\|^2 + \mathscr{E}_\tau(U^n, U^{n+1}) \tag{4.16}$$

with the discrepancy

$$\mathscr{E}_\tau(U^n,U^{n+1}) := 2\tau\sum_{i=1}^{q} b_i \operatorname{Re}(\dot U^{ni},U^{ni}). \tag{4.17}$$

Now, if the inner products $(\dot U^{ni},U^{ni}), i=1,\dots,q$, are imaginary, then the discrepancy $\mathscr{E}(U^n,U^{n+1})$ vanishes and the method is L^2-conservative, i.e., it satisfies (4.10), the discrete analogue of the first invariant (2.4). For the (nonlinear) SAV–Gauss methods, we have $\widetilde U^{ni} = U^{ni}, i=1,\dots,q$, in (4.7)–(4.8), and it is evident from the first relation of (4.7) that the inner products $(\dot U^{ni},U^{ni}) = -\mathrm{i}\|\nabla U^{ni}\|^2 + \mathrm{i}\lambda(R^{ni}W(U^{ni}),U^{ni}), i=1,\dots,q$, are indeed imaginary. We infer that the (nonlinear) SAV–Gauss methods for (2.13) are L^2-conservative. □

An immediate consequence of the proof of Theorem 4.1 is:

Corollary 4.1 (Energy preservation of the linearized SAV–Gauss methods) *The SAV method* (4.7)–(4.9) *with arbitrary* $\widetilde U^{ni}, i=1,\dots,q$, *satisfies a discrete analogue of* (2.8)*, namely*

$$E_\tau(U^{n+1},R^{n+1}) = E_\tau(U^n,R^n), \quad n=0,\dots,N-1. \tag{4.18}$$

Remark 4.2 (Method (4.7)–(4.9) *with arbitrary* $\widetilde U^{ni}$ *is not* L^2*-conservative)* Let us note that the SAV method (4.7)–(4.9) with arbitrary $\widetilde U^{ni}, i=1,\dots,q$, is, in general, not L^2-conservative.

Remark 4.3 (The linearized Crank–Nicolson method) The one-stage Gauss method is the midpoint or Crank–Nicolson method. Similarly, it is easily seen that the one-stage ($q=1$) method (4.7)–(4.9) can be written in the form

$$\begin{cases} \bar\partial U^{n+1} = \mathrm{i}\Delta U^{n+\frac12} + \mathrm{i}\lambda R^{n+\frac12} W\big(\frac12(\widetilde U^{n+1}+U^n)\big), \\ \bar\partial R^{n+1} = \frac12 \operatorname{Re}\big(W\big(\frac12(\widetilde U^{n+1}+U^n)\big),\bar\partial U^{n+1}\big), \end{cases} \quad n=0,\dots,N-1. \tag{4.19}$$

Of course, for $\widetilde U^{n+1} = U^{n+1}$, (4.19) reduces to the SAV–Crank–Nicolson method (4.1).

Testing the first equation of (4.19) against $\bar\partial U^{n+1}$, integrating by parts the first term on the right-hand side, and using the second equation of (4.19), we have

$$\|\bar\partial U^{n+1}\|^2 = -\mathrm{i}(\nabla U^{n+\frac12},\nabla\bar\partial U^{n+1}) + 2\mathrm{i}\lambda R^{n+\frac12}\bar\partial R^{n+1}. \tag{4.20}$$

Taking imaginary parts, we see that (4.19) is energy-conservative, as it satisfies the discrete analogue of the second invariance property (2.8), namely

$$\|\nabla U^{n+1}\|^2 - 2\lambda|R^{n+1}|^2 = \|\nabla U^n\|^2 - 2\lambda|R^n|^2, \quad n=0,\dots,N-1. \tag{4.21}$$

Furthermore, testing the first equation of (4.19) against $U^{n+\frac12}$ and integrating by parts the first term on the right-hand side, we have

$$(\bar\partial U^{n+1},U^{n+\frac12}) = -\mathrm{i}\|\nabla U^{n+\frac12}\|^2 + \mathrm{i}\lambda R^{n+\frac12}\big(W\big(\frac12(\widetilde U^{n+1}+U^n)\big),U^{n+\frac12}\big),$$

and thus, taking real parts,

$$\operatorname{Re}(\bar\partial U^{n+1},U^{n+\frac12}) = \lambda R^{n+\frac12}\operatorname{Im}\big(W\big(\frac12(\widetilde U^{n+1}+U^n)\big),U^{n+\frac12}\big),$$

whence

$$\|U^{n+1}\|^2 = \|U^n\|^2 + 2\lambda R^{n+\frac{1}{2}} \operatorname{Im}\big(W\big(\frac{1}{2}(\widetilde{U}^{n+1}+U^n)\big), U^{n+\frac{1}{2}}\big). \tag{4.22}$$

Notice that from the second equation of (4.1) we only used the fact that $R^{n+\frac{1}{2}}$ is real.

Therefore, the discrete analogue of (2.4) is satisfies only if $\big(W\big(\frac{1}{2}(\widetilde{U}^{n+1}+U^n)\big), U^{n+\frac{1}{2}}\big)$ is real. One possibility is the nonlinear method, with $\widetilde{U}^{n+1} = U^{n+1}$; see §2.2.

Remark 4.4 (Other boundary conditions) It is evident from the derivation of the discrete invariance properties (4.10) and (4.11) that they are valid also for homogeneous Neumann boundary conditions as well as for periodic boundary conditions.

5 Numerical examples

We present results of several numerical experiments to illustrate our theoretical findings. In space we discretized by the finite difference method in the first, one-dimensional example, and used MATLAB, while in the second, two-dimensional example we discretized by the finite element method, and used the software Freefem.

Example 5.1 We consider the following one-dimensional NLS equation

$$u_t = 0.1\mathrm{i}u_{xx} + \mathrm{i}|u|^{p-1}u, \quad (x,t) \in [0,1]\times(0,100], \tag{5.1}$$

subject to homogeneous Dirichlet boundary conditions, with initial value

$$u^0(x) = \sin(\pi x).$$

We present results for $p = 5$ and for $p = 7$.

We performed our calculations in double precision. In space we discretized by the standard centered three-point finite difference method with spatial stepsize $h = 0.1$. For the temporal discretization of the original formulation of the NLS equation we used the linearized (extrapolated) Crank–Nicolson (ECN) method, corresponding to (4.19), the standard Crank–Nicolson (CN) method (3.1), as well as the modified Crank–Nicolson (MCN) method (3.8); in the ECN method we linearized by linearly extrapolating the values U^n and U^{n-1}, $\widetilde{U}^{n+1} := 2U^n - U^{n-1}$ and thus $(\widetilde{U}^{n+1}+U^n)/2 = 1.5U^n - 0.5U^{n-1}$, while the nonlinear CN and MCN methods were implemented by several fixed point iterations in the nonlinear term. We also employed the SAV–Crank–Nicolson (SAV–CN) method (4.1) to the SAV reformulated problem. All these methods yield nodal approximations U_j^n of the exact values $u(jh,t_n)$, $j = 0,\dots,J = 1/h$; the approximate solution U^n of $u(\cdot,t_n)$ is then the piecewise linear interpolant of $U_0^n,\dots,U_J^n$. The discrepancies M^n and D^n of the discrete mass (density) and energy, respectively, between the numerical solutions U^n and the starting value U^0, the piecewise linear interpolant of u^0,

$$M^n := |\|U^n\| - \|U^0\|| \quad \text{and} \quad D^n := |E(U^n) - E(U^0)|, \tag{5.2}$$

are presented in Figure 5.1–5.2 for various temporal stepsizes, for $p = 7$. Notice that D^n is the discrepancy of the original energy $E(U^n)$, even for the SAV methods, rather than of the modified energy $E_\tau(U^n,R^n)$. We can see that the discrepancies of the discrete mass are of the order of the machine precision for the CN, MCN and SAV–CN methods; in contrast, the

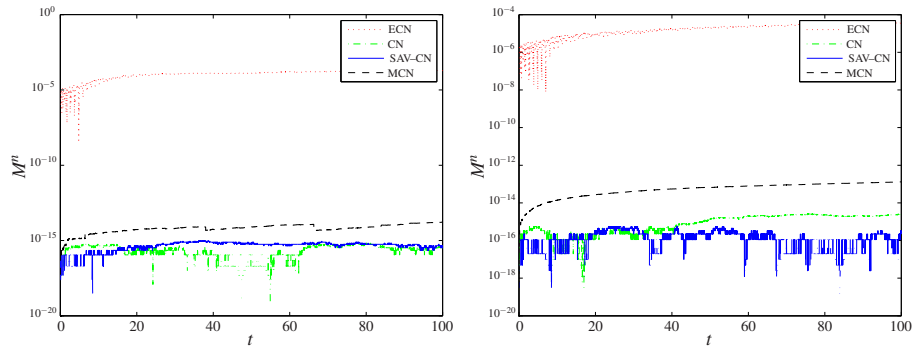

Fig. 5.1 Example 5.1: The discrepancies M^n of the discrete mass (density), see (5.2), for $p = 7$ and $\tau = 1/40$ (left) and $\tau = 1/80$ (right), for the extrapolated Crank–Nicolson, Crank–Nicolson, SAV–Crank–Nicolson and modified Crank–Nicolson methods.

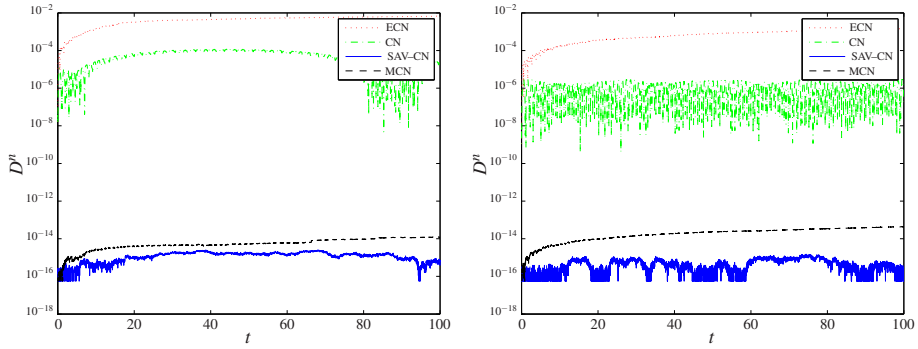

Fig. 5.2 Example 5.1: The discrepancies D^n of the discrete energy (Hamiltonian), see (5.2), for $p = 7$ and $\tau = 1/40$ (left) and $\tau = 1/80$ (right), for the extrapolated Crank–Nicolson, Crank–Nicolson, SAV–Crank–Nicolson and modified Crank–Nicolson methods.

discrepancies of the discrete energy are sufficiently small and remain nearly unchanged only for the modified Crank–Nicolson (MCN) method (3.8) and for the SAV–CN method (4.1).

Furthermore, we present the modulus of the numerical solutions by the extrapolated Crank–Nicolson, Crank–Nicolson, and SAV–Crank–Nicolson methods in Figure 5.3, as well as the modulus of the differences of the numerical solutions by the SAV–CN method from the numerical solutions by the ECN and CN methods, in the left and right panels of Figure 5.4, respectively. One can see that the differences between the solutions of these methods increase in time. These results indicate that the structure-preserving methods are more effective for long time simulations.

Next, we applied the two-stage Gauss and SAV–Gauss methods. The discrepancies of the discrete mass and energy are presented in Figures 5.5–5.6 for various temporal stepsizes, for $p = 5$. One can see that the discrepancies of mass for the Gauss and the SAV–Gauss methods as well as of the energy for the SAV–Gauss method are of the order of the machine precision.

These numerical results indicate that the SAV–CN and high-order SAV–Gauss methods are L^2-conservative and satisfy a discrete analogue of the energy conservation of the NLS equation; in contrast, the standard Gauss methods for the original formulation of the NLS are only L^2-conservative.

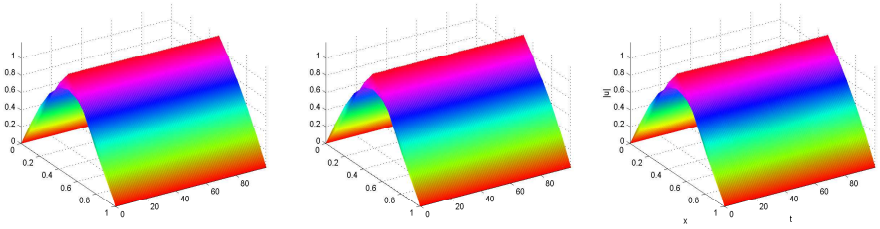

Fig. 5.3 Example 5: The modulus of the numerical solutions by the extrapolated Crank–Nicolson (left), Crank–Nicolson (middle), and SAV–Crank–Nicolson (right) methods.

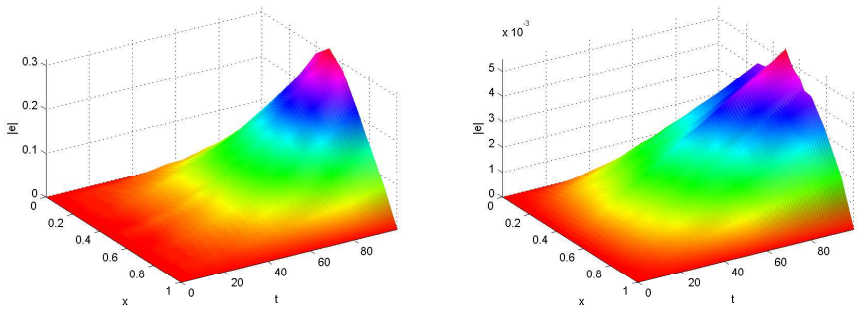

Fig. 5.4 Example 5: The modulus of the differences of the numerical solutions by the SAV–Crank–Nicolson method from the numerical solutions by the extrapolated Crank–Nicolson (left panel) and Crank–Nicolson (right panel) methods.

Finally, we tested the energy-conservation properties of the linearized SAV–Gauss methods. As in the case of the original form of the NLS equation, for the linearized one-stage SAV–Gauss (or SAV–Crank–Nicolson) method, see (4.19), $\widetilde{U}^{n+1}$ is obtained by linearly extrapolating the values U^n and U^{n-1}, $\widetilde{U}^{n+1} := 2U^n - U^{n-1}$. For the linearized two-stage SAV–Gauss method, $\widetilde{U}^{ni}, i = 1,2$, are computed by polynomial extrapolation of the values of the intermediate approximations $U^{n-1,i}, i = 1,2$, at the preceding time interval,

$$\text{(5.3)} \qquad \begin{cases} \widetilde{U}^{n1} = \dfrac{1}{c_2 - c_1} U^{n-1,2} - \Big(\dfrac{1}{c_2 - c_1} - 1\Big) U^{n-1,1} = \sqrt{3}\, U^{n-1,2} - \big(\sqrt{3} - 1\big) U^{n-1,1}, \\ \widetilde{U}^{n2} = \Big(1 + \dfrac{1}{c_2 - c_1}\Big) U^{n-1,2} - \dfrac{1}{c_2 - c_1} U^{n-1,1} = \big(1 + \sqrt{3}\big) U^{n-1,2} - \sqrt{3}\, U^{n-1,1}. \end{cases}$$

The discrepancies of the discrete mass and energy for various stepsizes are presented in Figures 5.7–5.8, for $p = 5$. The discrepancies of the discrete energy are of the order of the machine precision, while the discrepancies of the discrete mass vary with time. These results further confirm the conclusions in Remarks 4.1 and 4.3.

Example 5.2 We next consider the two-dimensional NLS equation

$$\text{(5.4)} \qquad u_t = \mathrm{i}(u_{xx} + u_{yy}) + \mathrm{i}|u|^3 u, \quad (x,y,t) \in [0,1] \times [0,1] \times (0,100],$$

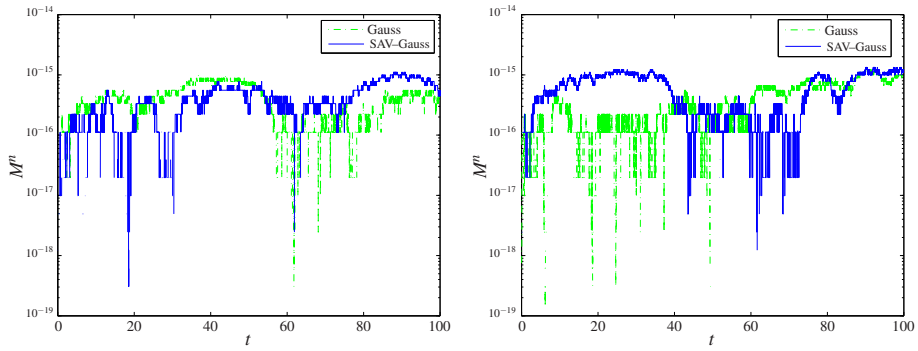

Fig. 5.5 Example 5.1: The discrepancies M^n of the discrete mass (density), see (5.2), for $p = 5$ and $\tau = 1/40$ (left) and $\tau = 1/80$ (right), for the two-stage Gauss and SAV–Gauss methods.

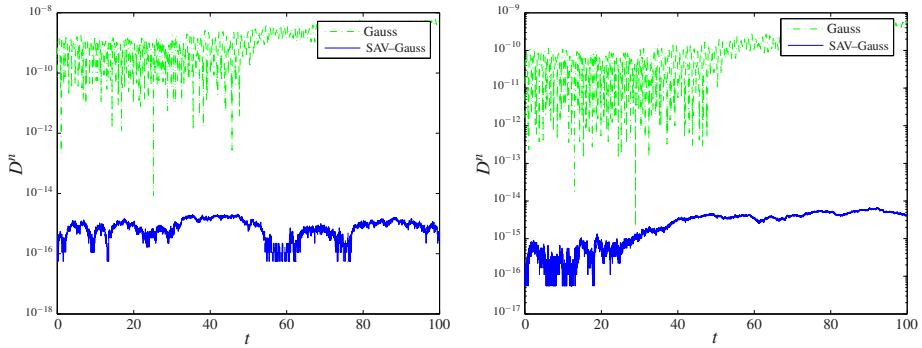

Fig. 5.6 Example 5.1: The discrepancies D^n of the discrete energy (Hamiltonian), see (5.2), for $p = 5$ and $\tau = 1/40$ (left) and $\tau = 1/80$ (right), for the two-stage Gauss and SAV–Gauss methods.

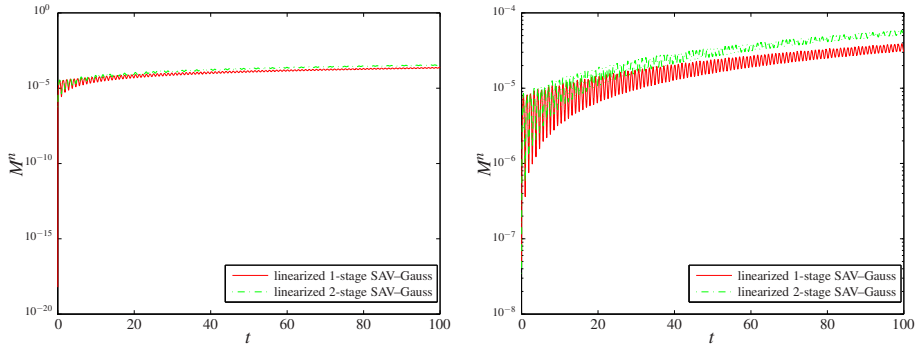

Fig. 5.7 Example 5.1: The discrepancies M^n of the discrete mass (density), see (5.2), for $p = 5$ and $\tau = 1/40$ (left) and $\tau = 1/80$ (right), for the linearized one- and two-stage Gauss and SAV–Gauss methods.

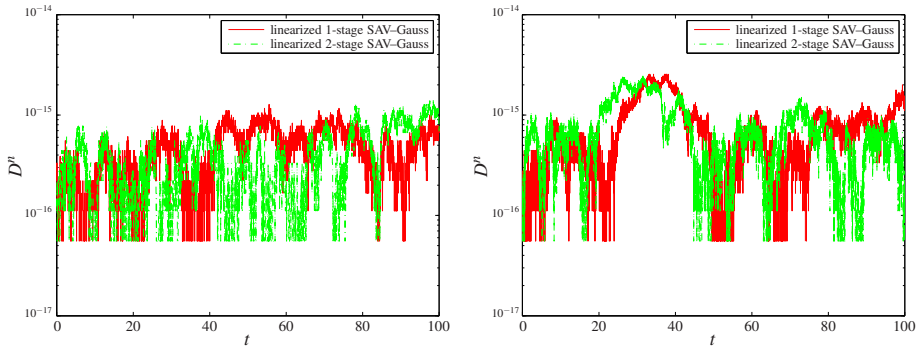

Fig. 5.8 Example 5.1: The discrepancies D^n of the discrete energy (Hamiltonian), see (5.2), for $p = 5$ and $\tau = 1/40$ (left) and $\tau = 1/80$ (right), for the linearized one- and two-stage Gauss and SAV–Gauss methods.

subject to homogeneous Dirichlet boundary conditions, with initial value

$$u^0(x,y) = x^2(1-x)^2y^2(1-y)^2.$$

For the space discretization we used the software Freefem with linear finite elements and a uniform triangular mesh with 11 nodes in each direction; the linear solver uses the generalized minimal residual (with tolerance 10^{-16}). In time we first discretized by the extrapolated Crank–Nicolson method, the Crank–Nicolson method (3.1) and the SAV–Crank–Nicolson method (4.1), respectively. The discrepancies M^n and D^n of the discrete mass (density) and energy, are presented in Figure 5.9–5.10 for various temporal stepsizes. Notice that D^n is the discrepancy of the original energy $E(U^n)$, even for the SAV methods, rather than of the modified energy $E_\tau(U^n, R^n)$. We can see that the discrepancies of the discrete mass are less than 10^{-15} for both the Crank–Nicolson and SAV–Crank–Nicolson methods; in contrast, the discrepancies of the discrete energy are sufficiently small and remain nearly unchanged only for the SAV–Crank–Nicolson method.

We also present the modulus of the SAV–Crank–Nicolson approximations in Figure 5.11 as well as the modulus of the differences of the SAV–Crank–Nicolson approximations from the extrapolated Crank–Nicolson and the Crank–Nicolson approximations in Figures 5.12 and 5.13, respectively. Again, the differences between these approximations increase as the time increases. These results further confirm the effectiveness of the structure-preserving methods for long time simulations.

6 Conclusions

It is well known that the Gauss methods for the nonlinear Schrödinger (NLS) equation are L^2-conservative but are not energy-conservative. In this article, we used the scalar auxiliary variable (SAV) reformulation of the NLS equation and constructed classical, L^2-conservative SAV–Gauss methods satisfying a discrete analogue of the energy conservation property. An important advantage of these structure-preserving methods is that they exhibit improved long time behavior. We also developed computationally advantageous linearizations of the base SAV–Gauss methods and discussed their conservation properties. The extrapolated linearly implicit variants are not L^2-conservative; consequently, they are not suitable for long time simulations.

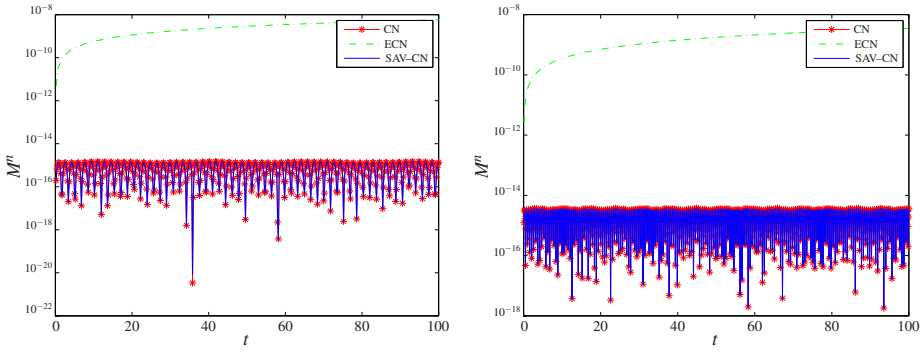

Fig. 5.9 Example 5.2: The discrepancies M^n of the discrete mass (density), see (5.2), for $\tau = 1/5$ (left) and $\tau = 1/10$ (right), for the extrapolated Crank–Nicolson, Crank–Nicolson, and SAV–Crank–Nicolson methods.

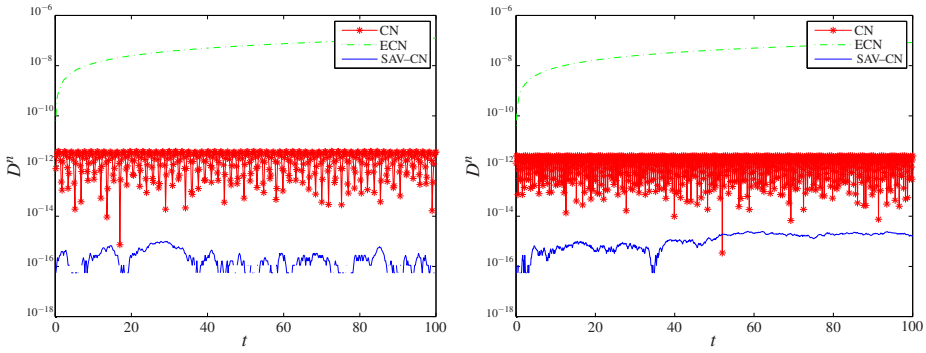

Fig. 5.10 Example 5.2: The discrepancies D^n of the discrete energy (Hamiltonian), see (5.2), for $\tau = 1/5$ (left) and $\tau = 1/10$ (right), for the extrapolated Crank–Nicolson, Crank–Nicolson, and SAV–Crank–Nicolson methods.

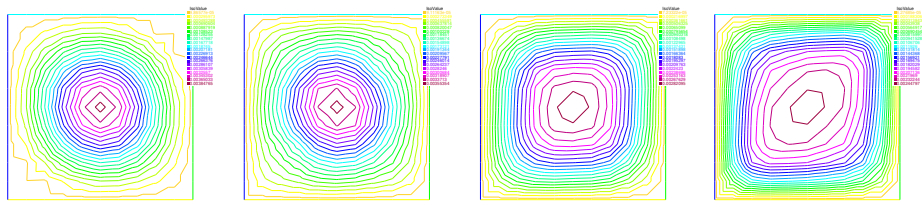

Fig. 5.11 Example 5.2: The modulus of the SAV–Crank–Nicolson approximations at $t = 10, 40, 70, 100$ (from left to right) for $\tau = 1/10$.

References

1. G. B. Agrawal, *Nonlinear Fiber Optics*, 3rd ed., Academic Press, London, 2001.
2. G. D. Akrivis, V. A. Dougalis, and O. A. Karakashian, *On fully discrete Galerkin methods of second-order temporal accuracy for the nonlinear Schrödinger equation*, Numer. Math. **59** (1991) 31–53.
3. G. Akrivis, V. A. Dougalis, and O. Karakashian, *Solving the systems of equations arising in the discretization of some nonlinear p.d.e.'s by implicit Runge–Kutta methods*, (RAIRO:) Math. Model. Numer. Anal. **31** (1997) 251–287.

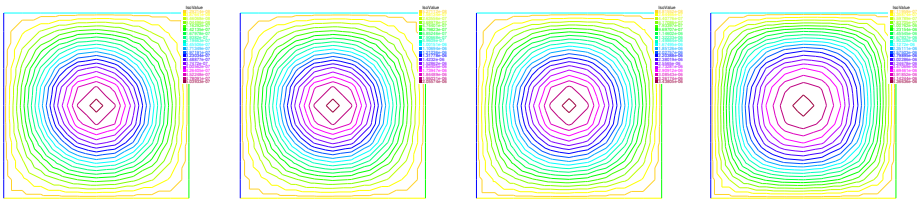

Fig. 5.12 Example 5.2: The modulus of the differences between the extrapolated Crank–Nicolson FEM approximations and the SAV–Crank–Nicolson FEM approximations at $t = 10, 40, 70, 100$ (from left to right) for $\tau = 1/10$.

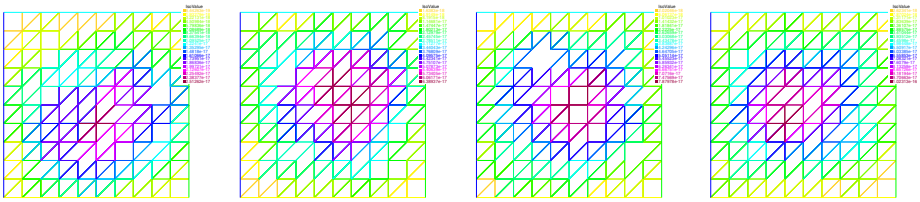

Fig. 5.13 Example 5.2: The modulus of the differences between the Crank–Nicolson FEM approximations and the SAV–Crank–Nicolson FEM approximations at $t = 10, 40, 70, 100$ (from left to right) for $\tau = 1/10$.

4. G. Akrivis, B. Li, and D. Li, *Energy-decaying extrapolated RK-SAV methods for the Allen–Cahn and Cahn–Hilliard equations*, SIAM J. Sci. Comput. **41** (2019) A3703–A3727.
5. L. Barletti, L. Brugnano, G. Frasca Caccia, and F. Iavernaro, *Energy-conserving methods for the nonlinear Schrödinger equation*, Appl. Math. Comput. **318** (2018) 3–18.
6. C. Besse, *Schéma de relaxation pour l' équation de Schrödinger non linéaire et les systèmes de Davey et Stewartson*, C. R. Acad. Sci. Paris Sér. I **326** (1998) 1427–1432.
7. C. Besse, *A relaxation scheme for the nonlinear Schrödinger equation*, SIAM J. Numer. Anal. **42** (2004) 934–952.
8. C. Besse, S. Descombes, G. Dujardin, and I. Lacroix-Violet, *Energy preserving methods for nonlinear Schrödinger equations*, IMA J. Numer. Anal. **41** (2021) 618–653.
9. H. Brezis and T. Gallouët, *Nonlinear Schrödinger evolution equations*, Nonlinear Anal. **4** (1980) 677–681.
10. L. Brugnano and F. Iavernaro, *Line Integral Methods for Conservative Problems*, Monographs and Research Notes in Mathematics, CRC Press, Boca Raton, FL, 2016.
11. L. Brugnano and F. Iavernaro, *Line integral solution of differential problems*, Axioms **7** (2018) 36.
12. L. Brugnano, F. Iavernaro, J. I. Montijano, and L. Rández, *Spectrally accurate space-time solution of Hamiltonian PDEs*, Numer. Algorithms **81** (2019) 1183–1202.
13. B. Cano and A. González-Pachón, *Projected explicit Lawson methods for the integration Schrödinger equation*, Numer. Meth. PDEs **31** (2015) 78–104.
14. E. Celledoni, D. Cohen, and B. Owren, *Symmetric exponential integrators with an application to the cubic Schrödinger equation*, Found. Comput. Math. **8** (2008) 303–317.
15. S. H. Christiansen, H. Z. Munthe-Kaas, and B. Owren, *Topics in structure-preserving discretization*, Acta Numer. **20** (2011) 1–119.
16. D. Cohen and L. Gauckler, *One-stage exponential integrators for nonlinear Schrödinger equations over long times*, BIT Numer. Math. **52** (2012) 877–903.
17. M. Delfour, M. Fortin, and G. Payre, *Finite-difference solutions of a non-linear Schrödinger equation*, J. Comput. Phys. **44** (1981) 277–288.
18. A. Durán and J. M. Sanz-Serna, *The numerical integration of relative equilibrium solutions. The nonlinear Schrödinger equation*, IMA J. Numer. Anal. **20** (2000) 235–261.
19. Z. Fei, V. M. Pérez-García, and L. Vázquez, *Numerical simulation of nonlinear Schrödinger systems: a new conservative scheme*, Appl. Math. Comput. **71** (1995) 165–177.
20. X. Feng, H. Liu, and S. Ma, *Mass- and energy-conserved numerical schemes for nonlinear Schrödinger equations*, Commun. Comput. Phys. **26** (2019) 1365–1396.

21. E. Hairer, C. Lubich, and G. Wanner, *Geometric Numerical Integration. Structure-Preserving Algorithms for Ordinary Differential Equations*, Reprint of the 2nd (2006) ed., Springer–Verlag, Heidelberg, Springer Series in Computational Mathematics v. 31, 2010.
22. E. Hairer and G. Wanner, *Solving Ordinary Differential Equations II*: *Stiff and Differential–Algebraic Problems*, 2nd revised ed., Springer–Verlag, Berlin Heidelberg, Springer Series in Computational Mathematics v. 14, 2002.
23. O. Karakashian, G. D. Akrivis, and V. A. Dougalis, *On optimal–order error estimates for the nonlinear Schrödinger equation*, SIAM J. Numer. Anal. **30** (1993) 377–400.
24. O. Karakashian and C. Makridakis, *A space-time finite element method for the nonlinear Schrödinger equation*: *the continuous Galerkin method*, SIAM J. Numer. Anal. **36** (1999) 1779–1807.
25. M. Knöller, A. Ostermann, and K. Schratz, *A Fourier integrator for the cubic nonlinear Schrödinger equation with rough initial data*, SIAM J. Numer. Anal. **57** (2019) 1967–1986.
26. D. Li and W. Sun, *Linearly implicit and high–order energy–conserving schemes for nonlinear wave equations*, J. Sci. Comput. **65** (2020) 83.
27. I. Mitra and S. Roy, *Relevance of quantum mechanics in circuit implementation of ion channels in brain dynamics*, Preprint, https://arxiv.org/abs/q-bio/0606008v1.
28. T. Ogawa, *A proof of Trudinger's inequality and its application to nonlinear Schrödinger equations*, Nonlinear Anal. **14** (1990) 765–769.
29. A. Osborne, *Nonlinear Ocean Waves and the Inverse Scattering Transform*, Academic Press, Burlington, MA, 2010.
30. H. L. Pécseli, *Waves and Oscillations in Plasmas*, CRC Press, Boca Raton, FL, 2013.
31. J. J. Rasmussen and K. Rypdal, *Blow-up in nonlinear Schrödinger equations*–I: *A general review*, Phys. Scripta **33** (1986) 481–497.
32. J. M. Sanz-Serna, *Runge–Kutta schemes for Hamiltonian systems*, BIT **28** (1988) 877–883.
33. J. Shen and J. Xu, *Convergence and error analysis for the scalar auxiliary variable* (*SAV*) *schemes to gradient flows*, SIAM J. Numer. Anal. **56** (2018) 2895–2912.
34. J. Shen, J. Xu, and J. Yang, *The scalar auxiliary variable* (*SAV*) *approach for gradient flows*, J. Comput. Phys. **353** (2018) 407–416.
35. W. A. Strauss, *The nonlinear Schrödinger equation*, In: Contemporary Developments in Continuum Mechanics and Partial Differential Equations, G. M. de la Penha and L. A. J. Medeiros, eds., pp. 452–465. North–Holland, New York, 1978.
36. W. A. Strauss, *Nonlinear Wave Equations*, AMS, Providence, RI, 1993.
37. W. A. Strauss and L. Vazquez, *Numerical solution of a nonlinear Klein–Gordon equation*, J. Comput. Phys. **28** (1978) 271–278.
38. C. Sulem and P.–L. Sulem, *The Nonlinear Schrödinger Equation, Self-Focusing and Wave Collapse*, Springer Verlag, New York, 1999.
39. X. Yang, *Linear, first and second-order, unconditionally energy stable numerical schemes for the phase field model of homopolymer blends*, J. Comput. Phys **327** (2016) 294–316.
40. X. Yang and L. Ju, *Efficient linear schemes with unconditional energy stability for the phase field elastic bending energy model*, Comput. Meth. Appl. Mech. Engrg. **315** (2017) 691–712.
41. G. E. Zouraris, *On the convergence of a linear two-step finite element method for the nonlinear Schrödinger equation*, M^2AN Math. Model. Numer. Anal. **35** (2001) 389–405.
42. G. E. Zouraris, *Error estimation of the relaxation finite difference scheme for a nonlinear Schrödinger equation*, Preprint, http://arxiv.org/abs/2002.09605v1.